Reduction of Unphysical Wave Reflection Arising from Space-Time Finite Integration Method

Tetsuji Matsuo and Takeshi Mifune
Graduate School of Engineering, Kyoto University
Nishikyo-ku, Kyoto, 615-8510, Japan
tmatsuo@kuee.kyoto-u.ac.jp

***Abstract*—Several 3D and 4D space-time grids are compared for electromagnetic wave computation by space-time finite integration method. An improved approximation of constitutive relation is proposed to suppress unphysical wave-reflection. The computational accuracy resulting from several space-time grids are numerically compared.**

***Index Terms*—Computational electromagnetics, finite difference methods, time domain analysis.**

I. Introduction

The finite integration (FI) method [1]-[4] achieves time-domain electromagnetic wave computation on unstructured spatial grid. Similarly to the FDTD method, the FI method uses a uniform time-step, which is restricted by the CFL condition with respect to the smallest spatial grid size. Refs. [5], [6] developed a space-time FI method to introduce non-uniform time-steps on 3D and 4D space-time grids. However, it was found that nonuniform spatial grid construction may cause unphysical wave-reflection. Refs. [7] and [8] proposed improved 3D and 4D space-time grids to suppress the unphysical wave-reflection due to the grid nonuniformity. This study proposes another space-time grid with an improved expression of constitutive relation based on a vectorial correction. The computational accuracy resulting from several space-time grids are compared.

II. Finite Integration Method on a Space–Time Grid

The coordinate system is denoted by $(ct, x, y, z) = (x^0, x^1, x^2, x^3)$ where $c = 1 / \sqrt{(\varepsilon_0\mu_0)}$, and ε_0 and μ_0 are the electric and magnetic constants. The integrated form of Maxwell equations are given as:

$$\oint_{\partial\Omega_\mathrm{p}} F = 0\,,\ \oint_{\partial\Omega_\mathrm{d}} G = \int_{\Omega_\mathrm{d}} J \tag{1}$$

$$F = -\textstyle\sum_{i=1}^{3} E_i \mathrm{d}x^0\mathrm{d}x^i + \sum_{j=1}^{3} \mathcal{B}_j \mathrm{d}x^k\mathrm{d}x^l,$$
$$G = \textstyle\sum_{i=1}^{3} H_i \mathrm{d}x^0\mathrm{d}x^i + \sum_{j=1}^{3} \mathcal{D}_j \mathrm{d}x^k\mathrm{d}x^l,$$
$$J = c\rho \mathrm{d}x^1\mathrm{d}x^2\mathrm{d}x^3 - \textstyle\sum_{j=1}^{3} J_j \mathrm{d}x^0\mathrm{d}x^k\mathrm{d}x^l \tag{2}$$

where $(\mathcal{B}_1, \mathcal{B}_2, \mathcal{B}_3) = c\boldsymbol{B}$ and $(\mathcal{D}_1, \mathcal{D}_2, \mathcal{D}_3) = c\boldsymbol{D}$; (j, k, l) is a cyclic permutation of (1, 2, 3); Ω_p and Ω_d are hypersurfaces in space-time. The boundaries $\partial\Omega_\mathrm{p}$ and $\partial\Omega_\mathrm{d}$ are represented by the faces of primal and dual grids in the FI method. The electromagnetic variables are defined in the FI method as:

$$f = \int_{\mathrm{Sp}} F\,,\ g = \int_{\mathrm{Sd}} G \tag{3}$$

where $\mathrm{S_p}$ and $\mathrm{S_d}$ are the faces of primal and dual grids.

The Hodge dual grid [6] is used to express the constitutive equation simply as:

$$\int_{\mathrm{Sd}} c_\mathrm{r} \mathrm{d}x^0\mathrm{d}x^j \,/ \int_{\mathrm{Sp}} \mathrm{d}x^k\mathrm{d}x^l = -\int_{\mathrm{Sd}} \mathrm{d}x^k\mathrm{d}x^l \,/ \int_{\mathrm{Sp}} c_\mathrm{r} \mathrm{d}x^0\mathrm{d}x^j = a \tag{4}$$

where $c_\mathrm{r} = 1 / \sqrt{(\varepsilon_\mathrm{r}\mu_\mathrm{r})}$, a is a constant determined for each pair of $\mathrm{S_p}$ and $\mathrm{S_d}$; ε_r and μ_r are the specific permittivity and permeability. Thereby, $f = Zg / a$ is obtained, where $Z = \sqrt{(\mu_\mathrm{r}\mu_0/\varepsilon_\mathrm{r}\varepsilon_0)}$ is the impedance.

III. 3D-Space-Time Grid with 2D Space

Fig. 1 illustrates space-time grids proposed in this paper, where domains (I) and (II) have uniform time-steps Δx^0 and $\Delta x^0/2$, respectively; domain (III) is the connecting domain. Figs. 2(a) and (b) show the grid structure of corner parts of domain (III) examined in [5] and [8], respectively. The former grid causes unphysical wave-reflection because of spatial irregularity whereas the latter suppresses the unphysical wave reflection using an improved constitutive relation. However, inaccuracy due to the corner structure was not removed completely. The grids shown in Fig. 2(a), 2(b) and Fig. 1 are called types A, B and C, respectively, in this article.

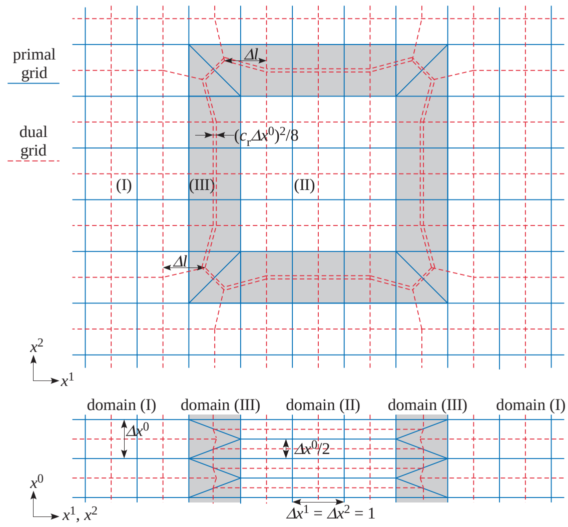

Fig. 1. Space-time grid (solid line: primal grid, dashed lines: dual grid).

Type C grid has dual edges that are not orthogonal to corresponding primal faces as shown in Fig. 1. This study examines two types of constitutive relations described by Eqs. (5) and (6).

$$e_{xi} = \varepsilon_\mathrm{r}\varepsilon_0\, d_{xi} / \Delta l\,,\ e_{yi} = \varepsilon_\mathrm{r}\varepsilon_0\, d_{yi} / \Delta l\ \ (i = 1, 2) \tag{5}$$

$$e_{xi} = \varepsilon_\mathrm{r}\varepsilon_0\, (d_{xi} + d_{xy}/2)\,,\ e_{yi} = \varepsilon_\mathrm{r}\varepsilon_0\, (d_{yi} + d_{xy}/2)\ \ (i = 1, 2) \tag{6}$$

where d and e are the electric flux and the integration of electric field given by (3), respectively. Based on the vectorial correction illustrated in Fig. 3, (6) gives more accurate approximation of constitutive relation than Eq. (5). The extended paper will discuss the numerical stability of space-time FI scheme based on the eigenvalue analysis of impedance matrix with relations (5) and (6).

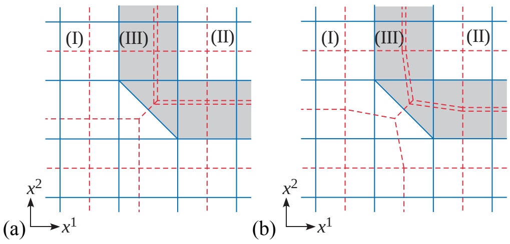

Fig. 2. Corner of Domain (III): (a) type A grid and (b) type B grid.

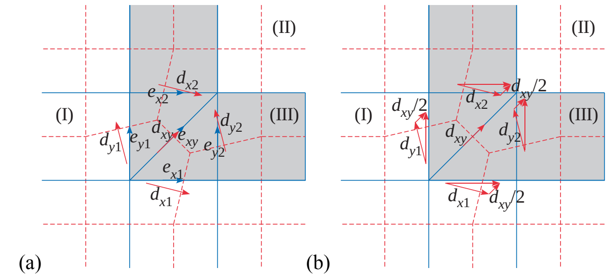

Fig. 3. Corner of domain (III) of type C grid: (a) variables and (b) vectorial correction.

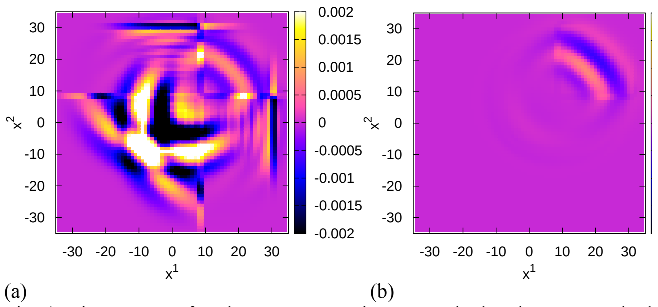

Fig. 4. Discrepancy of $\mathcal{B}_3$ between space-time FI method and FDTD method: (a) type A grid, and (b) type C grid with (9).

Fig. 4 portrays distributions of discrepancy $\Delta\mathcal{B}_3$ between $\mathcal{B}_3$ obtained in the same way as in [8] by the FDTD method and the FI method with type A and C grids. The type A grid yields numerical error whereas the numerical error is suppressed by the type C grid with (6) type relation. The comparison with the type B grid and another grid [7] will be reported in the extended paper.

IV. 4D-Space-Time Grid with 3D Space

Fig. 5 illustrates 4D space-time grids of type C at the corner of domain (III). A wave propagation is simulated similarly to [6], where electromagnetic wave is scattered by a cubic pore with $\varepsilon_r = 1$ surrounded by dielectric with $\varepsilon_r = 5$. Figs. 6(a)-(d) portray distributions of $\mathcal{B}_3$ given by (a) the FDTD method (b) the space-time FI method using type B grid with correction similar to (6), (c) with type C grid and (5), and (d) with type C grid and (6). The FDTD method uses the same uniform spatial grid and time-step as in domain (II) and requires about two times as much computation time as the space-time FI method. Compared with Fig. 6(a), small inaccuracy is observed behind the pore in Fig. 6(b) even with correction similar to (6). The type C grid with (6) achieves accurate computation as in Fig. 6(d). The numerical instability is not observed even after $x^0 = 10^5\Delta x^0$. The comparison with another 4D grid [7] with 3D corners of domain (III) will be reported in the extended paper.

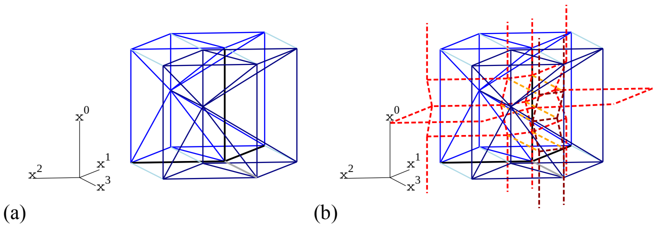

Fig. 5. 4D Space-time grid of type C where solid and dashed lines represent primal and dual grids: (a) primal grid, and (b) primal and dual grids.

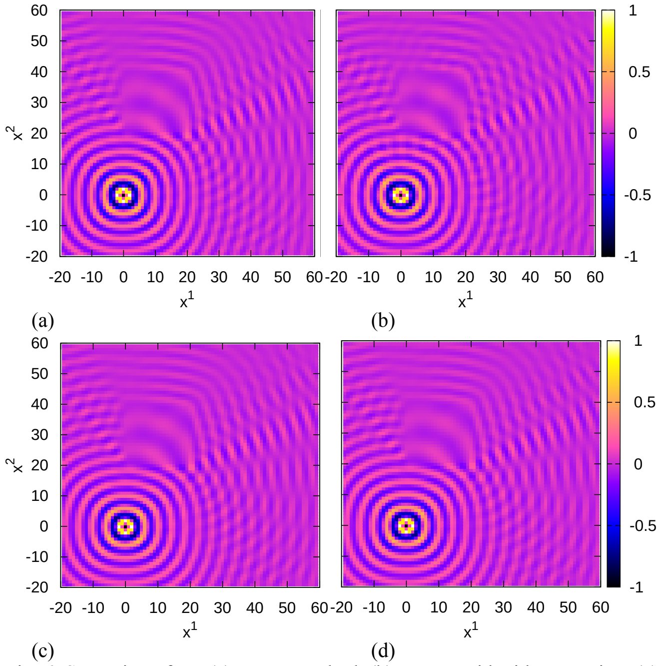

Fig. 6. Scattering of $\mathcal{B}_3$: (a) FDTD method, (b) type B grid with correction, (c) type C grid with relation (5), and type C grid with relation (6).

References

[1] T. Weiland, "Time domain electromagnetic field computation with finite difference methods," *Int. J. Numer. Model.,* vol. 9, pp. 295-319, 1996.

[2] I. E. Lager, E. Tonti, A.T. de Hoop, G. Mur, and M. Marrone, "Finite formulation and domain-integrated field relations in electromagnetics - a synthesis," *IEEE Trans. Magn.*, vol. 39, pp. 1199-1202, 2003.

[3] P. Alotto, A. De Cian, and G. Molinari, "A time-domain 3-D full-Maxwell solver based on the cell method," *IEEE Trans. Magn.*, vol. 42, pp. 799-802, 2006.

[4] L. Codecasa and M. Politi, "Explicit, consistent, and conditionally stable extension of FD-TD to tetrahedral grids by FIT," *IEEE Trans. Magn.*, vol. 44, pp. 1258-1261, 2008.

[5] T. Matsuo, "Electromagnetic field computation using space-time grid and finite integration method," *IEEE Trans. Magn.*, vol. 46, pp. 3241-3244, 2010.

[6] T. Matsuo, "Space-time finite integration method for electromagnetic field computation," *IEEE Trans. Magn.*, vol. 47, pp. 1530-1533, 2011.

[7] T. Matsuo, S. Shimizu, and, T. Mifune, "3D and 4D space-time grids for electromagnetic wave computation using finite integration method," APS-URSI Chicago , 362.3, 2012.

[8] T. Matsuo, and, T. Mifune, "3D and 4D space-time grids for electromagnetic field analysis using finite integration method," JSST 2012 Intl. Conf. Simulation Technology, OS1, 2012.